

Received June 18, 2019, accepted July 12, 2019, date of publication July 23, 2019, date of current version August 7, 2019.

Digital Object Identifier 10.1109/ACCESS.2019.2930688

A Dual-Band Microwave Filter Design for Modern Wireless Communication Systems

JIANCHUN XU^{1,3}, KE BI^{1,3}, XIAOJUN ZHAI², YANAN HAO¹,
AND KLAUS D. MCDONALD-MAIER²

¹State Key Laboratory of Information Photonics and Optical Communications, School of Science, Beijing University of Posts and Telecommunications, Beijing 100876, China

²School of Computer Science and Electronic Engineering, University of Essex, Colchester CO4 3SQ, U.K.

³Research Institute, Beijing University of Posts and Telecommunications, Shenzhen 518057, China

Corresponding authors: Ke Bi (bike@bupt.edu.cn) and Xiaojun Zhai (xzhai@essex.ac.uk)

This work was supported in part by the National Natural Science Foundation of China under Grant 61774020, Grant 51802023, Grant 11574311, and Grant 51802021, in part by the Science and Technology Plan of Shenzhen City under Grant JCYJ20180306173235924, and in part by the Ph.D. student short-term overseas study and exchange program of BUPT, China.

ABSTRACT Nowadays, modern communication system relies on the designs of high-performance devices to enhance communication effect for a high quality of life and smart city system. As a crucial signal processing step, microwave filter removes unwanted frequency components away from the received signal and enhances the useful ones. However, large loss, bulky size, and single-band greatly limit the practical applications in urban computing. Therefore, the filters with dual-band characteristic are highly desirable for modern wireless communication, such as device-to-device communication, environment monitoring, and automatic driving. In this paper, a dual-band microwave filter is designed and fabricated based on the theory of Mie-resonance extraordinary transmission. An electromagnetic wave cannot propagate through a subwavelength aperture drilled in a metallic film. By adding two dielectric cuboids of different sizes into the two apertures, two passbands appear in the frequency range of 10.0–12.0 GHz. In this range, the insertion loss is less than 0.4 dB, and 3-dB bandwidth is more than 48 MHz. Particularly, the two passband frequencies can be tuned by adjusting the size of the dielectric cuboids. This approach opens a way for designing tunable dual-band microwave bandpass filter, which is benefit for enhancing spectrum resource utilization.

INDEX TERMS Dual-band, extraordinary transmission, microwave filter, modern wireless communication.

I. INTRODUCTION

With the development of modern wireless communication technology, the device-to-device communications (D2D), digital world, intelligent devices, etc. have been popular research areas in recent years [1]–[3]. All these emerging technologies would need the sustains of highly efficient signal processing components. As a crucial part of the signal processing components, the filters play an important role in such wireless communication systems.

In the D2D communication, portable devices can directly communicate with others by the D2D communication, avoiding the utilization of a traditional cellular network [4]. However, the leakage interference makes the synchronization of D2D transmission impossible [5]. Therefore, the filters are desired to limit the leakage power and minimized the amount of transmission information for good spectrum properties.

The associate editor coordinating the review of this manuscript and approving it for publication was Lu Liu.

Regarding the digital world and environment monitoring, the filters perform initial bandwidth limiting and have a strong impact on the information acquisition and the processing of the information [6], [7]. The filters affect both the capacity of the sending data and frequency range. Thus, the filters often are used as a method of improving the quality of service. Even in the volume visualization, the low pass filter can smooth the details on the image.

The development of new technology and new concept often bring more stringent requirements on the devices [8], [9]. The conventional filters pose a fundamental obstacle for the modern applications owing to their high insertion loss, single band, and complex structure [10]–[12]. A promising path to solve this problem is the utilization of new technology in the filter design.

Based on Bethe's theory, electromagnetic wave cannot propagate through a subwavelength aperture [13]. Since Ebbesen *et al.* [14]. obtained an enhanced transmission through subwavelength hole arrays by combining surface

plasmons and diffractive coupling effects, extraordinary transmission has inspired tremendous interests [15]. The underlying physics of this phenomenon is widely regarded to be related to the surface plasmons resonance that couples the aperture through the metal interface. Recently, many configurations have been theoretically and experimentally proposed to demonstrate the efficient extraordinary transmission [16], [17]. Besides surface plasmons resonance mode, the resonator coupling mode has also been designed and studied [18]. Two of the surprising features of extraordinary transmission with resonator coupling mode are that the radiating area is strongly confined to the vicinity of the resonators and the very high total transmission appears at a certain frequency. It is believed that this remarkable enhancement has novel technological applications such as sensing, near-field microscopy, light harvesting and microwave transmission filters [19].

With the rapid development of modern new technology, the new conceptions, such as digital world, smart cities artificial intelligence models, must bring forward higher requests to the signal processing. Therefore, the filters with high channel selectivity and dual/multi-band characteristics are strongly demanded [20]–[22]. In recent years, many studies have been carried out on the dual-band filters. Stepped impedance resonators and split rings are widely used to realize dual-band ability of the filter by changing the structural parameters [23], [24]. To miniaturize the structure of the dual-band filter, some approaches were proposed further. Tsai and Hsue put forward a dual-band bandpass filter by using equal-length coupled-serial-shunted microstrip line structure [25]. Our group studied a dual-band bandstop filter based on ferrite metamaterials [26], [27]. However, most of them have relative high insertion loss and complex structures. The Mie resonances of dielectric particles provide a novel mechanism for the creation of magnetic or electric resonance and offer a simpler and more versatile route for the fabrication of multiband devices [28]. Very recently, Mie-resonance extraordinary transmission has drawn intense attentions due to its low loss and high transmission enhancement [29]. In this work, we demonstrate a dual-band microwave filter based on Mie-resonance extraordinary transmission. The remainder of this paper is organized as follows. Section II presents the design of the proposed filter structure. In Section III the simulated and measured results of the dual-band filter are exhibited and the tuning principle is discussed. Section IV draws the conclusion of his paper.

II. STRUCTURAL DESIGN

Figure 1 shows the schematic diagrams of the dual-band Mie-resonance extraordinary transmission-based microwave filter. As shown in Fig. 1(a), two subwavelength apertures with a diameter of $D = 3.2$ mm are perforated on a metallic film of thickness $t = 1$ mm. The size of the metallic film is set as 22.86×10 mm² for the utilization in waveguide. In order to facilitate the establishment of the model, the distance between the two apertures of A1 and A2 is 10 mm. To realize the

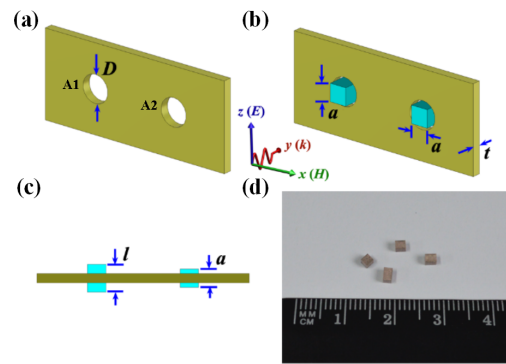


FIGURE 1. Schematic diagrams of the dual-band Mie-resonance extraordinary transmission-based microwave filter. (a) Metallic plate with two subwavelength apertures. (b) Perspective view and (c) cross-section (yx -plane) of two dielectric cuboids placed in the apertures. (d) Photograph of the fabricated dielectric cuboids.

extraordinary transmission, two dielectric cuboids are placed in the apertures. Figure 1b and 1c show the perspective view and cross-section (yx -plane) of two dielectric cuboids placed in the apertures. The dielectric cuboids are CaTiO₃-based ceramic that doped with 2 wt.% Zr₂O. The permittivity and loss tangent of the dielectric cuboids are 124 and 0.002, respectively. The ceramic is sliced into two dielectric cuboids with dimensions of $a \times a \times a$ mm³ and $l \times a \times a$ mm³, where a is 2.0 mm, the length l of the dielectric cuboid in the aperture of A1 is 2.0 mm, 2.2 mm, 2.6 mm and 3.0 mm, respectively. The photograph of the fabricated dielectric cuboids are shown in Fig. 1(d).

The numerical predictions of the transmission properties are performed by the commercial CST Microwave Studio. The boundary conditions of the x and z directions are set as electric ($E_t = 0$), and the boundary condition of y direction is open. Figure 2(a) shows the simulated transmission spectrum for the metallic plate with two subwavelength apertures. Figure 2(b) shows the simulated transmission spectra for the dielectric cuboid with a series of length l . The insets are the schematic diagram of the simulation setup for the dielectric cuboid. Based on Mie resonance theory, at the first resonance the dielectric resonator is equivalent to a magnetic dipole within the long-wavelength limit. Owing to the magnetic Mie-resonance, a transmission dip appears in the range of 9.5 - 12.0 GHz. As the length l of the dielectric cuboid increases from 2.0 mm to 3.0 mm, the resonance frequency decreases from 11.5 GHz to 10.1 GHz. The Mie-resonance frequency of a rectangular cavity resonator with metal walls can be described as [30]

$$f = \frac{1}{2\sqrt{\epsilon\mu}} \sqrt{\left(\frac{m}{w}\right)^2 + \left(\frac{n}{l}\right)^2 + \left(\frac{p}{h}\right)^2} \quad (1)$$

where integers m , n and p are the number of half wave variations in the x , y and z directions, respectively; w , l and h are the wide, length and height of the dielectric resonator in the x , y and z directions, respectively; ϵ and μ are the permittivity and permeability of the resonator, respectively. According to (1), the magnetic Mie-resonance frequency can be

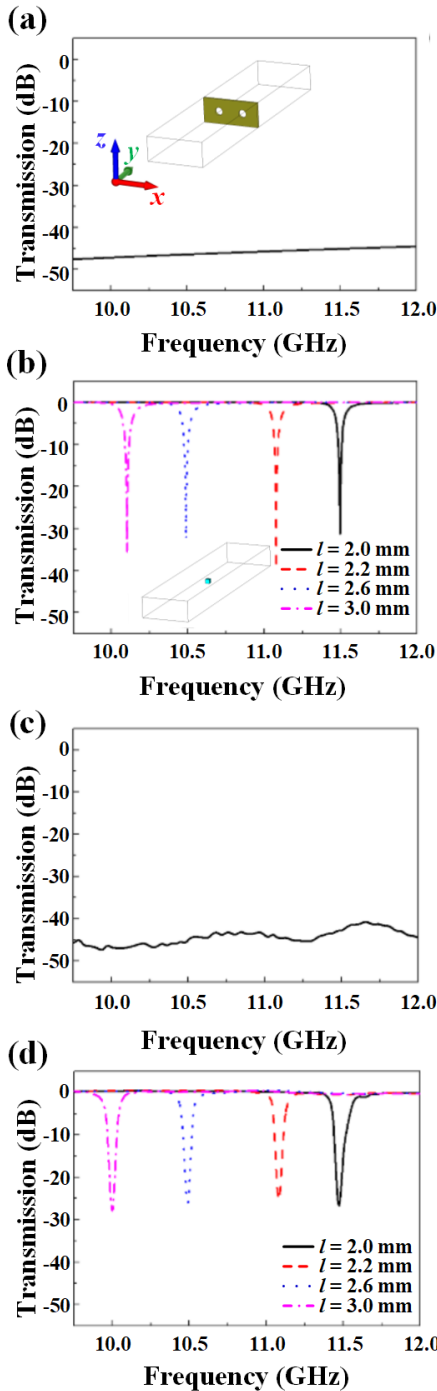


FIGURE 2. (a) Simulated transmission spectrum for the metallic plate with two subwavelength apertures. (b) Simulated transmission spectra for the second dielectric cuboid with a series of length l . The insets show the schematic diagrams of the simulation setups. (c) Measured transmission spectrum for the metallic plate with two small apertures. (d) Measured transmission spectra for the second dielectric cuboid with a series of length l .

influenced by the size of the dielectric resonator. The resonance frequency will decrease as the l increases. Obviously, the theoretical predictions agree with the simulated results shown in Fig. 2(b). The microwave measurement system is composed of a vector network analyzer (HP 8720ES)

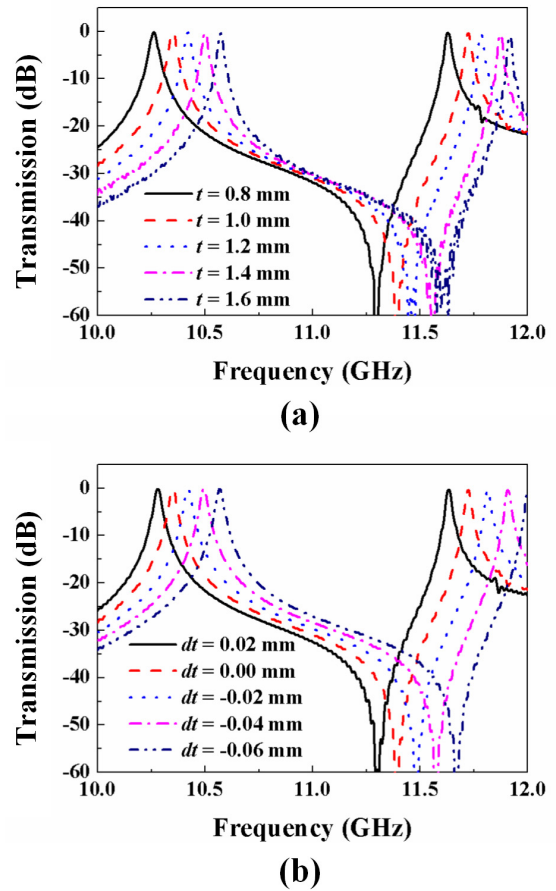


FIGURE 3. (a) Simulated transmission spectrum for the proposed filter with a series of thickness t . (b) Simulated transmission spectrum for the length variation of the two dielectric cuboids.

and two X-band rectangular waveguides (WR90, $22.86 \times 10.16 \text{ mm}^2$). The microwave with TE₁₀ mode propagates along with y axis, the electric field direction and magnetic field direction of normal incident wave is along with z axis and x axis, respectively. Figure 2(c) and 2(d) show the measured transmission spectra for the metallic plate with two small apertures and the dielectric cuboid with a series of length l , respectively. One can see that the measured results are in good agreement with the simulated ones. Based on the size effect of the dielectric cuboid, a filter with dual-band property is designed.

In addition to the above simulations, the thickness t of the metallic film is also an important parameter. Figure 3(a) shows the simulated transmission spectra of the proposed filter with various metallic film thickness t . From this figure, the transmission spectra curve shifts to high frequency as a result of increasing the thickness. However, the metallic film with two apertures can't transmit electromagnetic wave. Thus, this changing of transmission spectra is possibly occurred by altering the relative position between the dielectric cuboids and the metallic film. To verify this suppose, the simulated transmission spectrum for the length variation of the two dielectric cuboids are depicted in the Fig. 3(b). As shown in this figure, altering two dielectric

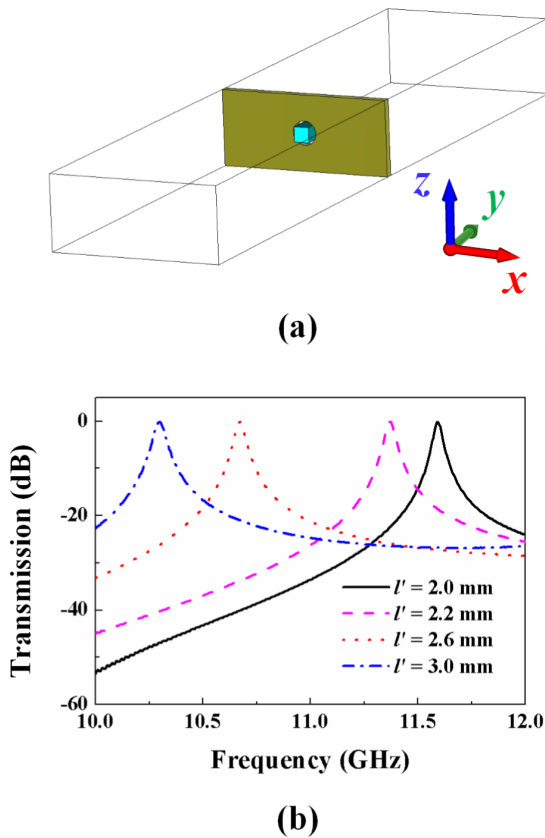


FIGURE 4. (a) Schematic diagram of the filter with single aperture. (b) Simulated transmission spectrum for the single-aperture filter with a series of length l' .

cuboids' lengths can realize the same effect as changing the metallic film thickness, which demonstrates the above predictions. Moreover, this method is more regular and obtains larger adjustable range.

III. RESULTS AND DISCUSSION

Firstly, the electromagnetic response to the filter with single aperture is discussed. The schematic diagram of the single-aperture filter is shown in Fig. 4(a). All parameters are same as Fig. 1(a) except the single aperture structure. Figure 4(b) shows the simulated transmission spectra for the filters with a series of cuboid length l' . As l' increases from 2.0 mm to 3.0 mm, the center frequency of the single-aperture filter decreases from 11.59 GHz to 10.30 GHz, coinciding well with the Mie-resonance theory (a rectangular cavity resonator).

Fig. 5(a) shows the schematic diagram of the simulation setup for the dual-band Mie-resonance extraordinary transmission-based microwave filter. The parameters in the simulations are consistent with that in the measurements. Fig. 5(b) shows the simulated transmission spectra for the filters with one and two dielectric cuboids. It can be seen that the bandwidth of the passband for the filter with two dielectric cuboids is much broader than that for the filter with one dielectric cuboid. The Simulated transmission spectra for the filter with a series of cuboid length l are shown in Fig. 5(c).

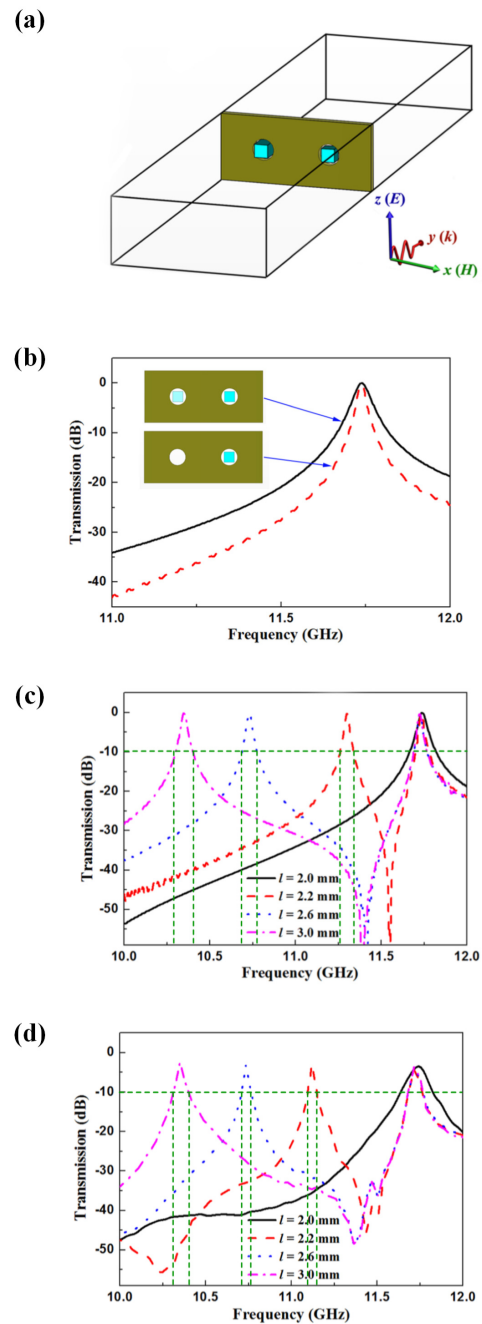


FIGURE 5. (a) Schematic diagram of the simulation setup for the dual-band Mie-resonance extraordinary transmission-based microwave filter. (b) Simulated transmission spectra for the filters with one and two dielectric cuboids. (c) Simulated and (d) measured transmission spectra for the filter with a series of length l .

The size of one cuboid is fixed. When the length of the second cuboid is the same as that of the first cuboid ($l = 2.0$ mm), a passband appears at 11.74 GHz. When $l > 2.0$ mm, two passbands appear in the frequency range of 10.0 - 12.0 GHz. It can be seen that the center frequency of one passband still locates around 11.74 GHz, while the center frequency of the other one decreases from 11.30 GHz to 10.35 GHz as l increases from 2.2 mm to 3.0 mm, which demonstrates a frequency tunable behavior. Moreover, the bandwidths of

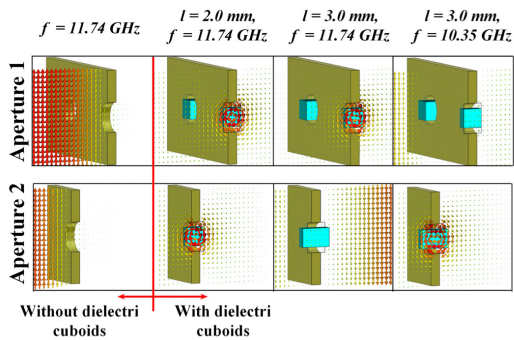


FIGURE 6. Simulated cross-sectional electric field distributions for the two apertures.

these passbands are 11.26 – 11.34 GHz, 10.69 – 10.78 GHz, and 10.30 - 10.40 GHz, respectively. The dual-band Mie-resonance extraordinary transmission-based microwave filters were placed into the waveguides to measure the transmission property. Figure 5(d) shows the measured transmission spectra for the filter with a series of length l . A passband appears at 11.73 GHz when $l = 2.0$ mm. As l increases from 2.2 mm to 3.0 mm, one passband frequency is 11.72 GHz, the other passband frequency decreases from 11.12 GHz to 10.35 GHz. And the measured values are 11.09 – 11.15 GHz, 10.70 – 10.76 GHz, and 10.31 – 10.39 GHz, respectively. The measured results agree well with the simulated ones. Due to the simple structure, the proposed filter mainly has dielectric loss of the dielectric cuboids. When $l = 3.0$ mm, the transmission coefficients are -2.5 dB and -3.5 dB for the frequencies of 10.35 GHz and 11.74 GHz. The measured results are in good agreements with the simulated ones, which confirms the prediction that the filter has dual-band and frequency tunable behaviors.

In order to figure out the underlying physics of the above phenomenon, we simulated the electric field distributions of the proposed filter. The upper and lower four maps in Fig. 6 illustrate the cross-sectional electric field distributions for the apertures A1 and A2, respectively. The length of the dielectric particle placed in aperture A2 is constant. Without the dielectric cuboids, the microwave cannot propagate through the subwavelength apertures (shown in the first column of two maps). From two maps in the second column, we can see that the electromagnetic fields are extremely localized at the two dielectric cuboids and the microwave can propagate through the subwavelength apertures. Because the length of the second cuboid is the same as that of the first one ($l = 2.0$ mm), magnetic Mie-resonances of the two dielectric cuboids occur at the same frequency of 11.74 GHz. Combined with the result shown in Fig. 3(b), one can see that only one passband appears in the frequency range of 10.0 GHz - 12.0 GHz and the bandwidth of this passband is enhanced. The two maps in the third column show the electric field distributions of the filter with $l = 3.0$ mm at 11.74 GHz. It can be seen that the Mie-resonance takes place in the first dielectric cuboid placed in aperture 1 and there are no electromagnetic fields localized at the second

dielectric cuboid. The two maps in the fourth column show the electric field distributions of the filter with $l = 3.0$ mm at 10.35 GHz. There are no electromagnetic fields localized at the first dielectric cuboid and the Mie-resonance takes place in the second dielectric cuboid placed in aperture 2. Because two Mie-resonances occur at two different frequencies, two passbands appear in the frequency range of 10.0 - 12.0 GHz. Based on the above results, we can know that the passbands of the proposed filter are induced by the Mie-resonance of the dielectric cuboids. The first dielectric cuboid placed in aperture 1 plays an important role in the passband at 11.74 GHz and the second dielectric cuboid placed in aperture 2 plays a key role in the passband at 10.35 GHz. Hence, the passband frequencies can be tuned by adjusting the size of the dielectric particles. Based on the above analyses, this design can be used in special frequency selective device.

IV. CONCLUSION

A Mie-resonance extraordinary transmission-based dual-band microwave filter is designed and fabricated for satisfying the demands of modern communication. The Mie-resonance frequency of the dielectric cuboid can be controlled by the cuboid size. By placing two dielectric cuboids of different sizes into the subwavelength metallic apertures, dual-band characteristic is realized. Both the simulated and measured results show that the passband frequencies can be tuned by adjusting the size of the dielectric cuboids. Moreover, the low loss and dual-band characteristics can effectively improve the signal quality and reduce the amount of data sent to the following stage to lower dynamic power, which is benefit for improving service quality of the D2D communication, smart city and intelligent devices. This work provides a way to fabricate microwave bandpass filters that have great potential for promoting the development of modern wireless communication systems in urban computing and intelligence applications.

REFERENCES

- [1] G. Fodor, S. Roger, N. Rajatheva, S. B. Slimane, T. Svensson, P. Popovski, J. M. Da Silva, and S. Ali, "An overview of device-to-device communications technology components in METIS," *IEEE Access*, vol. 4, pp. 3288–3299, 2016.
- [2] T. S. J. Darwish and K. A. Bakar, "Fog based intelligent transportation big data analytics in the Internet of vehicles environment: Motivations, architecture, challenges, and critical issues," *IEEE Access*, vol. 6, pp. 15679–15701, 2018.
- [3] W. Qu, Y. Zhang, H. Liu, T. Dou, J. Wang, Z. Li, S. Yang, and H. Ma, "Multi-party ring quantum digital signatures," *J. Opt. Soc. Amer. B*, vol. 36, no. 5, p. 1335, 2019.
- [4] T. Huynh, T. Onuma, K. Kuroda, M. Hasegawa, and W. J. Hwang, "Joint downlink and uplink interference management for device to device communication underlying cellular networks," *IEEE Access*, vol. 4, pp. 4420–4430, 2016.
- [5] Z. Zhou, C. Gao, C. Xu, T. Chen, D. Zhang, and S. Mumtaz, "Energy-efficient stable matching for resource allocation in energy harvesting-based device-to-device communications," *IEEE Access*, vol. 5, pp. 15184–15196, 2017.
- [6] F. J. Harris, C. Dick, and M. Rice, "Digital receivers and transmitters using polyphase filter banks for wireless communications," *IEEE Trans. Microw. Theory Techn.*, vol. 51, no. 4, pp. 1395–1412, Apr. 2003.

- [7] E. S. Hussein, M. Eslami, E. S. Hussein, M. S. Filali, S. T. Shalaby, A. Amira, F. Bensaali, S. Dakua, J. Abinayed, A. Al-Ansari, and A. Z. Ahmed, "Real-time automated image segmentation technique for cerebral aneurysm on reconfigurable system-on-chip," *J. Comput. Sci.*, vol. 27, pp. 35–45, Jul. 2018.
- [8] Y. Lu, L. Liu, J. Panneerselvam, X. Zhai, X. Sun, and N. Antonopoulos, "Latency-based analytic approach to forecast cloud workload trend for sustainable datacentres," *IEEE Trans. Sustain. Comput.*, to be published.
- [9] X. Bai, Z. Zhang, L. Liu, X. Zhai, J. Panneerselvam, and L. Ge, "Enhancing localization of mobile robots in distributed sensor environments for reliable proximity service applications," *IEEE Access*, vol. 7, pp. 28826–28834, 2019.
- [10] I. C. Hunter, L. Billonet, B. Jarry, and P. Guillon, "Microwave filters-applications and technology," *IEEE Trans. Microw. Theory Techn.*, vol. 50, no. 3, pp. 794–805, Mar. 2002.
- [11] H. Xu, K. Bi, Y. Hao, J. Zhang, J. Xu, J. Dai, K. Xu, and J. Zhou, "Switchable complementary diamond-ring-shaped metasurface for radome application," *IEEE Antennas Wireless Propag. Lett.*, vol. 17, no. 12, pp. 2494–2497, Dec. 2018.
- [12] K. Bi, X. Wang, Y. Hao, M. Lei, G. Dong, and J. Zhou, "Wideband slot-coupled dielectric resonator-based filter," *J. Alloys Compounds*, vol. 785, pp. 1264–1269, May 2019.
- [13] H. A. Bethe, "Theory of diffraction by small holes," *Phys. Rev. Lett.*, vol. 66, nos. 7–8, pp. 163–182, Oct. 1944.
- [14] T. W. Ebbesen, H. J. Lezec, H. F. Ghaemi, T. Thio, and P. A. Wolf, "Extraordinary optical transmission through sub-wavelength hole arrays," *Nature*, vol. 391, pp. 667–669, Feb. 1998.
- [15] L. Martín-Moreno, F. J. García-Vidal, H. J. Lezec, A. Degiron, and T. W. Ebbesen, "Theory of highly directional emission from a single subwavelength aperture surrounded by surface corrugations," *Phys. Rev. Lett.*, vol. 90, pp. 167401-1–167401-4, Apr. 2003.
- [16] S. S. Akarca-Biyikli, I. Bulu, and E. Ozbay, "Enhanced transmission of microwave radiation in one-dimensional metallic gratings with sub-wavelength aperture," *Appl. Phys. Lett.*, vol. 85, no. 7, pp. 1098–1100, Aug. 2004.
- [17] R. Gordon, A. G. Brolo, A. McKinnon, A. Rajora, B. Leathem, and K. L. Kavanagh, "Strong polarization in the optical transmission through elliptical nanohole arrays," *Phys. Rev. Lett.*, vol. 92, no. 3, 2004, Art. no. 037401.
- [18] Y. Guo and J. Zhou, "Dual-band-enhanced transmission through a sub-wavelength aperture by coupled metamaterial resonators," *Sci. Rep.*, vol. 5, Jan. 2015, Art. no. 8144.
- [19] J. R. Choi, K. Kim, Y. Oh, A. L. Kim, S. Y. Kim, J. S. Shin, and D. Kim, "Extraordinary transmission-based plasmonic nanoarrays for axially super-resolved cell imaging," *Adv. Opt. Mater.*, vol. 2, no. 1, pp. 48–55, Jan. 2014.
- [20] J. Xu, Y. Hao, K. Bi, R. Zhang, S. Huang, and J. Zhou, "Microwave orbital angular momentum beam generation based on circularly polarized metasurface antenna array," *Eng. Sci.*, vol. 6, pp. 30–35, Oct. 2019.
- [21] X. Gao, M. Zhao, M. Xie, M. Lei, X. Song, K. Bi, Z. Zheng, and S. Huang, "2D optically controlled radio frequency orbital angular momentum beam steering system based on a dual-parallel Mach-Zehnder modulator," *Opt. Lett.*, vol. 44, no. 2, p. 255, 2019.
- [22] M.-Y. H. and S.-M. Wang, "Compact and wideband microstrip band-stop filter," *Microw. Opt. Technol. Lett.*, vol. 50, no. 10, pp. 2612–2614, Oct. 2008.
- [23] W. Jiang, W. Shen, T. Wang, Y. M. Huang, Y. Peng, and G. Wang, "Compact dual-band filter using open/short stub loaded stepped impedance resonators (OSLSIRs/SSLIRs)," *IEEE Microw. Wireless Compon. Lett.*, vol. 26, no. 9, pp. 672–674, Sep. 2016.
- [24] Y. Xie, F.-C. Chen, and Z. Li, "Design of dual-band bandpass filter with high isolation and wide stopband," *IEEE Access*, vol. 5, pp. 25602–25608, 2017.
- [25] B. Ren, T. Zhang, J. Bao, D. Bukuru, and M. A. Khan, "Compact dual-band differential bandpass filter using quadruple-mode stepped-impedance square ring loaded resonators," *IEEE Access*, vol. 6, pp. 21850–21858, Apr. 2018.
- [26] K. Bi, W. Zhu, M. Lei, and J. Zhou, "Magnetically tunable wideband microwave filter using ferrite-based metamaterials," *Appl. Phys. Lett.*, vol. 106, Apr. 2015, Art. no. 173507.
- [27] K. Bi, D. Yang, J. Chen, Q. Wang, H. Wu, C. Lan, and Y. Yang, "Experimental demonstration of ultra-large-scale terahertz all-dielectric metamaterials," *Photon. Res.*, vol. 7, no. 4, p. 457, 2019.
- [28] Q. Zhao, J. Zhou, F. Zhang, and D. Lippens, "Mie resonance-based dielectric metamaterials," *Mater. Today*, vol. 12, no. 12, pp. 60–69, Dec. 2009.
- [29] Y. S. Guo, J. Zhou, C. W. Lan, H. Y. Wu, and K. Bi, "Mie-resonance-coupled total broadband transmission through a single subwavelength aperture," *Appl. Phys. Lett.*, vol. 104, May 2014, Art. no. 204103.
- [30] J. Kim and A. Gopinath, "Simulation of a metamaterial containing cubic high dielectric resonators," *Phys. Rev. B - Condens. Matter Mater. Phys.*, vol. 76, Sep. 2007, Art. no. 115126.



JIANCHUN XU received the B.S. degree in measurement and control technology and instrumentation program from the Beijing Institute of Technology, Beijing, China, in 2014. He is currently pursuing the Ph.D. degree with the School of Science, Beijing University of Posts and Telecommunications, Beijing. His research interests include orbital angular momentum antenna and broadband antenna.



KE BI received the Ph.D. degree from the Nanjing University of Aeronautics and Astronautics, in 2012. From 2012 to 2014, he was an Assistant Researcher with Tsinghua University. He is currently an Associate Professor with the Beijing University of Posts and Telecommunications. His research interests include information functional materials and devices, and electromagnetic metamaterials and devices.



XIAOJUN ZHAI received the B.Sc. degree from the North China University of Technology, China, in 2006, and the M.Sc. degree in embedded intelligent systems and the Ph.D. degree from the University of Hertfordshire, U.K., in 2009 and 2013, respectively. He is currently a Lecturer with the School of Computer Science and Electronic Engineering, University of Essex. His research interests mainly include the design and implementation of the digital image and signal processing algorithms, custom computing using FPGAs, embedded systems, and hardware/software codesign. He is also a BCS member and HEA Fellow.



YANAN HAO received the Ph.D. degree from Tsinghua University, in 2016. She is currently an Associate Professor with the Beijing University of Posts and Telecommunications. Her research interests include nano-scaled perovskite materials and their application in microelectronics and energy storage, and information functional materials and devices.



KLAUS D. MCDONALD-MAIER is currently the Head of the Embedded and Intelligent Systems Laboratory, University of Essex, Colchester, U.K. He is also the Chief Scientist with UltraSoC Technologies Ltd., the CEO of Metrarc Ltd., and a Visiting Professor with the University of Kent. His current research interests include embedded systems and system-on-chip design, security, development support and technology, parallel and energy-efficient architectures, computer vision, data analytics, and the application of soft computing and image processing techniques for real-world problems. He is also a member of VDE and a Fellow of the IET.